

Research Article

Performance Investigations of Quasi-Yagi Loop and Dipole Antennas on Silicon Substrate for 94 GHz Applications

Osama M. Haraz,^{1,2} Mohamed Abdel-Rahman,³ Najeeb Al-Khali,⁴
Saleh Alshebeili,^{1,3,4} and Abdel Razik Sebak^{1,5}

¹KACST Technology Innovation Center in Radiofrequency and Photonics for the e-Society (RFTONICS),
King Saud University, Riyadh 11451, Saudi Arabia

²Electrical Engineering Department, Faculty of Engineering, Assiut University, Assiut 71515, Egypt

³Prince Sultan Advanced Technologies Research Institute (PSATRI), College of Engineering,
King Saud University, Riyadh 11421, Saudi Arabia

⁴Electrical Engineering Department, King Saud University, P.O. Box 800, Riyadh 11421, Saudi Arabia

⁵Department of Electrical and Computer Engineering, Concordia University, Montreal, QC, Canada H3G 1M8

Correspondence should be addressed to Osama M. Haraz; osama_m_h@yahoo.com

Received 27 August 2014; Revised 20 November 2014; Accepted 22 November 2014; Published 8 December

Academic Editor: Kerim Guney

Copyright © 2014 Osama M. Haraz et al. This is an open access article distributed under the Creative Commons Attribution License, which permits unrestricted use, distribution, and reproduction in any medium, provided the original work is properly cited.

This paper introduces the design and implementation of two high gain Quasi-Yagi printed antennas developed on silicon substrate for 94 GHz imaging applications. The proposed antennas are based on either driven loop or dipole antennas fed by a coplanar waveguide (CPW) feeding structure. For better matching with the driven antennas, a matching section has been added between the CPW feedline and the driven antenna element. To improve the gain of either loop or dipole antennas, a ground reflector and parasitic director elements have been added. Two Quasi-Yagi antenna prototypes based on loop and dipole antenna elements have been fabricated and experimentally tested using W-band probing station (75–110 GHz). The measured results show good agreement with simulated results and confirm that the proposed antennas are working. In addition, a feed and matching configuration is proposed to enable coupling a microbolometer element to the proposed Quasi-Yagi antenna designs for performing radiation pattern measurements.

1. Introduction

In recent years, the printed Yagi-Uda antennas have attracted much interest with many applications in radar, millimeter-wave (MMW) imaging, wireless communication systems, phased arrays, and so forth. This is because they have many advantages such as wide bandwidth, high gain, low cost, end-fire radiation patterns, and ease of manufacturing and integration with other microwave circuits. In 1982, the printed Yagi-Uda antenna was introduced for the first time [1]. It consists of a driven element, a reflector, and one or more directors to create end-fire radiation characteristics. Presently, many researchers have exerted significant efforts to come up with several planar Yagi and Quasi-Yagi antenna designs to improve their performance [2–17]. One key factor

to obtain a wide operating bandwidth is the design of a suitable feed structure for these kinds of antennas.

A differentially fed high gain Yagi-Uda antenna with folded dipole feed was introduced in [2]. However, it has a bigger size along with degraded performance because of its complex feeding structure. A Quasi-Yagi antenna with a wide bandwidth of 74% and a gain of 4–8 dBi was proposed [3]. However, the asymmetry of those antennas also deteriorated their radiation performances. The complementary metal-oxide semiconductor transistor (CMOS) technology is used to design a CPW-fed on-chip Yagi-Uda antenna operating at 60 GHz [4]. However, a very low gain of –10 dB was achieved. In order to enhance the front-to-back ratio of the Quasi-Yagi antenna, another design based on a series-fed two-bowtie dipole array is presented [5]. In order to reduce the size of

Quasi-Yagi antenna, the Koch fractals (Sierpinski) shaped dipole elements are introduced [6]. In [7], in order to achieve the multiband operation for Yagi antenna, a driven dipole element is used with derived sections. Another design for a wideband Quasi-Yagi antenna with achievable bandwidth of 46% which is fed by microstrip-to-slot line transition is proposed [8]. In [9], a Quasi-Yagi antenna was designed to achieve a size reduction in the length of driver by using a folded dipole as a driven element. The proposed antenna has an achieved operational bandwidth of 1.3:1. A broadband planar Yagi antenna for millimeter-wave and submillimeter detectors has been proposed [10]. Another design for Quasi-Yagi antenna at 60 GHz is based on genetic algorithm (GA) to achieve a bandwidth of 16% [11]. Because of their high gain, an electrooptic (EO) wireless millimeter-wave-lightwave signal converter is proposed using planar Yagi-Uda array antennas coupled to resonant electrodes [12]. In [13], a novel wideband planar Quasi-Yagi antenna with a bandwidth of 48% and a gain of 6.2 dB using x-shaped elements is presented. A 60 GHz differential on-chip Quasi-Yagi antenna fabricated with $0.18 \mu\text{m}$ CMOS technology is proposed [14]. However, the achieved bandwidth is 33% and the gain is only -2.64 dB.

In this paper, two different Quasi-Yagi antennas utilizing either driven loop or dipole antennas are proposed. Two novel antenna designs, Yagi dipole and Yagi loop antennas, are proposed, manufactured, and measured. The proposed Quasi-Yagi antenna using elliptical loops instead of regular dipole elements is a novel design. The truncated ground plane of the antenna acts as a reflector for the transverse-electric surface wave generated by the driver. The parasitic directors are used to enhance the radiation in the forward end-fire direction. Novel feed and matching configuration to allow coupling a microbolometer element is proposed to enable a simple method for radiation pattern measurement. Two antenna prototypes have been fabricated and tested experimentally using a probing station. We also propose a novel feed and matching configuration to allow coupling a microbolometer element with the proposed Quasi-Yagi antennas for measuring the radiation patterns at 94 GHz. The simulated and measured results show that the antenna gain can reach 4 dBi and 8.1 dBi for prototypes I and II, respectively. The achieved beam width is of approximately 25° and 27° in XY plane ($\theta = 90^\circ$) and approximately 51° and 54° in YZ plane ($\phi = 90^\circ$) for prototypes I and II, respectively. The antenna radiation efficiency can reach 88% and 77% for prototypes I and II, respectively. Compared to other W-band millimeter-wave antennas fabricated on silicon substrates, our antennas are showing relatively higher gains.

2. The Proposed High Gain Quasi-Yagi Loop Antenna Prototype I

2.1. Antenna Geometry and Design. The geometrical configuration and seen structure of the proposed Quasi-Yagi loop antenna prototype I are introduced in Figure 1. The top view and side view of the proposed antenna are shown in Figures 1(a) and 1(b), respectively. The antenna is built on a silicon

TABLE 1: Optimized Quasi-Yagi loop antenna prototype I dimensions.

Parameter	Quantity	Value
A_1	Driven ellipse major radius	$928 \mu\text{m}$
B_1	Driven ellipse minor radius	$430 \mu\text{m}$
T_1	Driven ellipse thickness	$72 \mu\text{m}$
S_1	Spacing between the driven antenna and director 1	$1302 \mu\text{m}$
A_2	Director 1 ellipse major radius	$480 \mu\text{m}$
B_2	Director 1 ellipse minor radius	$280 \mu\text{m}$
T_2	Director 1 ellipse thickness	$72 \mu\text{m}$
S_2	Spacing between director 2 and director 1	$802 \mu\text{m}$
A_3	Director 2 ellipse major radius	$480 \mu\text{m}$
B_3	Director 2 ellipse minor radius	$280 \mu\text{m}$
T_3	Director 2 ellipse thickness	$72 \mu\text{m}$
W_G	Ground reflector width	$302 \mu\text{m}$
L_G	Ground reflector length	$1520 \mu\text{m}$
W	Substrate width	$3502 \mu\text{m}$
L	Substrate length	$5002 \mu\text{m}$
W_M	Matching section width	$564 \mu\text{m}$
L_M	Matching section length	$268 \mu\text{m}$
W_1	Interdigital capacitor width	$294 \mu\text{m}$
L_1	Interdigital capacitor length	$1052 \mu\text{m}$
W_F	CPW feedline width	$32 \mu\text{m}$
G	CPW feedline gap	$27 \mu\text{m}$
H_{Si}	Si substrate thickness	$380 \mu\text{m}$
H_{SiO_2}	SiO ₂ layer thickness	$1.2 \mu\text{m}$
H_{Al}	Al thickness	$0.2 \mu\text{m}$

dioxide (SiO₂) layer ($\epsilon_r = 4.84$) above a silicon (Si) substrate with $\epsilon_r = 11.7$. It consists of a driven elliptically shaped loop antenna, ground reflector (bigger in size), and two elliptically shaped parasitic loop directors (smaller in size) in front of the driven antenna. The antenna is fed using a coplanar waveguide (CPW) feeding structure. To improve the impedance matching between the driven antenna and the CPW feedline, a matching section has been utilized. Figure 1(c) presents the detailed view for matching section and CPW feedline. The optimized antenna parameters are calculated using extensive parametric studies and optimization techniques done in the full wave Computer Simulation Technology Microwave Studio (CST MWS) software program [18]. Table 1 summarized the optimized dimensions for the proposed Quasi-Yagi loop antenna prototype I.

2.2. Antenna Fabrication. The designed antennas are fabricated on a $385 \mu\text{m}$ thick high resistivity ($\rho > 5000 \Omega \text{cm}$) Si substrate. The Si substrate is coated on both sides with a $1.2 \mu\text{m}$ layer of SiO₂ for the purpose of electrical isolation. The following steps were performed for fabricating the printed antenna structures. First, a 200 nm layer of aluminum (Al) was deposited on the Si/SiO₂ substrate using direct current (DC) magnetron sputtering at 150 Watts of power, a chamber base pressure of 1.5×10^{-6} Torr, and an argon (Ar) pressure of 3 mTorr. Rohm & Haas S1813 photoresist was then spun at 4500 rpm for 60 sec. The photoresist was exposed for 4 sec at 175 Watts of ultraviolet power at a wavelength of

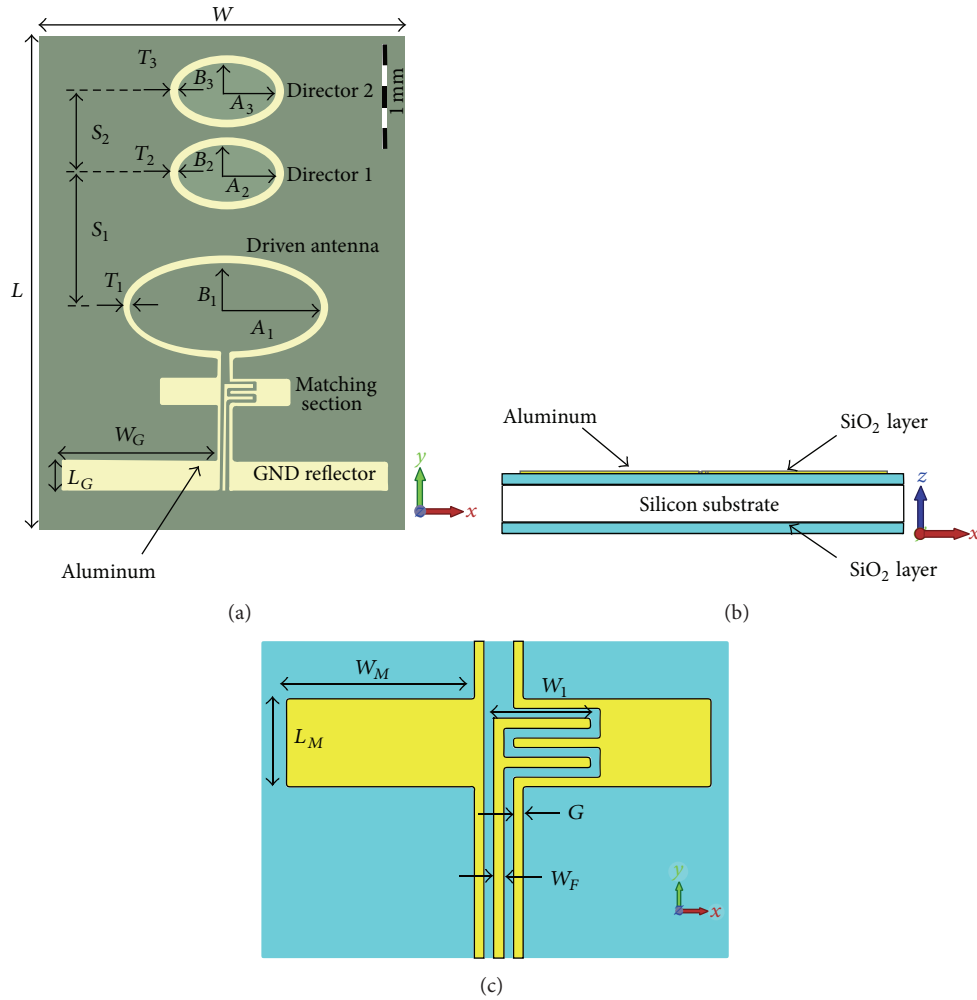


FIGURE 1: Geometrical configuration and photograph of the fabricated Quasi-Yagi loop antenna prototype I: (a) top view, (b) side view, and (c) detailed view for matching section and CPW feedline.

365 nm using an NXQ 4004 contact mask aligner. Next, a combined photoresist development and Al etching process was performed using Rohm & Haas MIF 319 developer. Aluminum was found to be etched by Rohm & Haas MIF 319 developer at an etch rate of 0.51 nm/s and so it was more practical to use Rohm & Haas MIF 319 developer for both photoresist development and Al etching processes. Rohm & Haas MIF 319 developer was applied for 9 minutes yielding resist-free and Al etched areas. Finally, the remaining photoresist was then removed using acetone. The fabricated Quasi-Yagi loop and dipole antennas are shown in Figures 1(a) and 6(a), respectively.

2.3. S-Parameter Measurement and Simulation. The $|S_{11}|$ versus frequency measurements were performed using Cascade Microtech's PM8 probe station in conjunction with Agilent E8361C network analyzer attached with N5260 frequency extender module, 67–110 GHz. Ground-signal-ground (GSG) infinity probes with a probe pitch of $75 \mu\text{m}$, connected to the frequency extender module, were accurately positioned on the CPW structures and then the $|S_{11}|$ versus frequency

measurements were performed at a frequency sweep from 80 to 110 GHz.

All simulations were carried out using Computer Simulation Technology Microwave Studio (CST-MWS) [8], which is considered a commercial and industry-standard full wave software program based on numerical analysis of electromagnetic problems. The measured and simulated $|S_{11}|$ curves versus frequency for the proposed Quasi-Yagi loop antenna prototype I are shown in Figure 2.

It can be seen that the shift in frequency between the simulated and measured cases is maybe because the substrates are not perfectly diced to the exact dimensions. Moreover, there may be some fabrication tolerance and calibration errors. In addition, the substrate dielectric properties are not correctly modeled in CST at those higher frequencies.

2.4. Radiation Pattern Measurement and Simulation. In this work, we propose coupling a microbolometer to the feed of the developed Quasi-Yagi loop antenna for performing radiation pattern measurements. For this purpose, a novel feed and matching section configuration is presented to permit

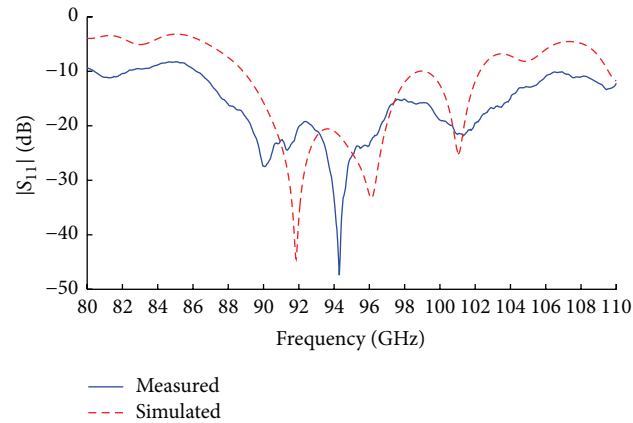


FIGURE 2: Measured and simulated reflection coefficient $|S_{11}|$ versus frequency of the proposed Quasi-Yagi loop antenna prototype I.

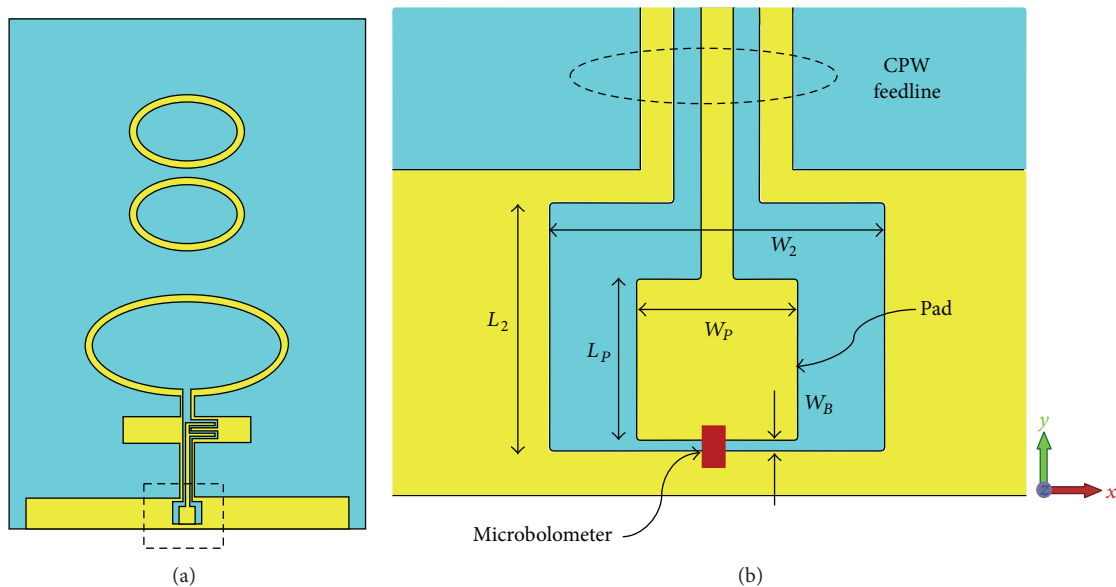


FIGURE 3: Geometrical configuration of the proposed Quasi-Yagi loop antenna prototype I with added microbolometer for radiation pattern measurements: (a) top view and (b) detailed view for bolometer.

coupling the microbolometer to the developed Quasi-Yagi loop antenna. In the meantime, the proposed design maintains similar radiation pattern characteristics to the original microbolometer-less Quasi-Yagi loop antenna design; this enables a proper comparison between both designs. The presented design in Figure 3 shows the developed antenna-coupled microbolometer configuration. The optimized parameters for the developed microbolometer are found to be as follows: $W_p (= L_p) = 152 \mu\text{m}$, $W_2 = 312 \mu\text{m}$, $L_2 = 232 \mu\text{m}$, and $W_B = 10 \mu\text{m}$. In the presented design, the CPW feedline, feeding the antenna signal to the microbolometer, is modified to include a square pad to permit biasing the microbolometer. This square pad allows connecting to one microbolometer terminal. The second microbolometer terminal will be connected to one section of the ground reflector. Bond wires will be connecting the square pad and the ground reflector to an external chip carrier.

The microbolometer material will be either niobium (Nb) or titanium (Ti) as they both possess the proper electrical resistivity for producing impedance matched loads within the constraints of the $10 \mu\text{m}$ feed gap (W_B) which will represent the length of the microbolometer. The width and thickness of the microbolometer structure will be exactly determined subsequent to a precise characterization of the electrical resistivity of the available material at the time of fabrication. The antenna resonant currents will be dissipated in the microbolometer located at the feed of the antenna causing joule heating in the microbolometer element. This joule heating will cause a resistance change in the microbolometer. A PIN switch will be used to modulate the MMW radiation incident on the microbolometer. The resistance change will be sensed by biasing the microbolometer element with a constant current and monitoring the voltage change. The voltage change will be monitored using a lock-in amplifier

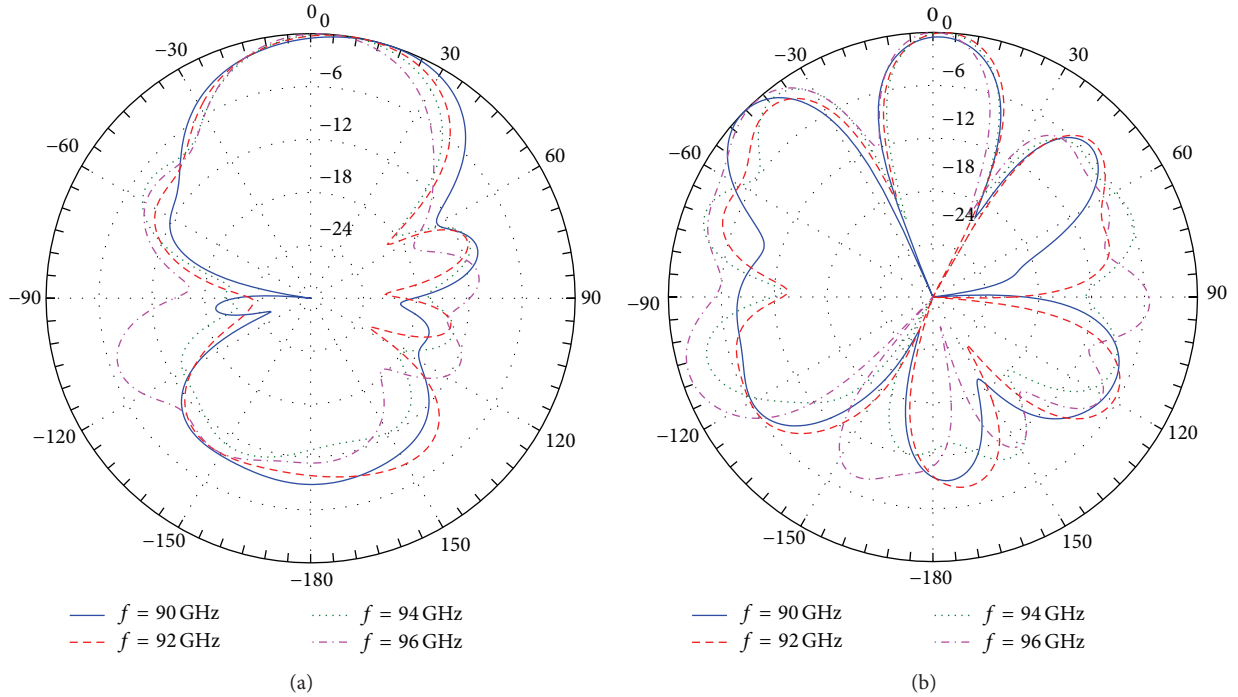


FIGURE 4: Simulated radiation patterns in (a) YZ plane and (b) XY plane at different frequencies $f = 90, 92, 94,$ and 96 GHz for the Quasi-Yagi loop array antenna prototype I.

referenced at the modulation frequency of the incident radiation.

The simulated antenna radiation patterns in both YZ plane ($\phi = 90^\circ$) and XY plane ($\theta = 90^\circ$) at different frequencies of 90, 92, 94, and 96 GHz are shown in Figures 4(a) and 4(b), respectively. In addition, the copolarization and cross-polarization components of the radiation patterns at 94 GHz in both planes Quasi-Yagi loop array antenna prototype II with and without microbolometer are calculated and presented in Figure 5. As shown from the simulated results, a good radiation pattern is achieved having a maximum gain of 6.5 dBi and side lobe level of -7.4 dB in YZ plane at frequency of 94 GHz. The 3 dB beam width is found to be approximately 51.2° ; furthermore, the antenna front-to-back ratio of 12.1 dB is achieved. The radiation characteristics in the XY plane are not as expected and they will be improved using the proposed Quasi-Yagi dipole antenna prototype II. The antenna peak-realized gain and radiation efficiency are calculated throughout the frequency band of interest. The results are given in the next section with a detailed comparison between the two antenna prototypes.

3. The Proposed High Gain Quasi-Yagi Dipole Antenna Prototype II

3.1. Antenna Configuration. The schematic diagram of the Quasi-Yagi dipole antenna prototype II is shown in Figure 6. In this case, the driven element is a printed dipole with two rectangular shaped directors in front of it. The optimized antenna parameters are tabulated in Table 2. The schematic

TABLE 2: Optimized Quasi-Yagi dipole antenna prototype II dimensions.

Parameter	Quantity	Value
A_1	Driven dipole length	$900 \mu\text{m}$
B_1	Driven dipole width	$400 \mu\text{m}$
S_1	Spacing between driven antenna and director 1	$1476 \mu\text{m}$
A_2	Director 1 rectangular length	$700 \mu\text{m}$
B_2	Director 1 rectangular width	$550 \mu\text{m}$
S_2	Spacing between director 1 and director 2	$1000 \mu\text{m}$
A_3	Director 2 rectangular length	$700 \mu\text{m}$
B_3	Director 2 rectangular width	$550 \mu\text{m}$
W_G	Ground reflector width	$300 \mu\text{m}$
L_G	Ground reflector length	$1520 \mu\text{m}$
W	Substrate width	$3500 \mu\text{m}$
L	Substrate length	$5000 \mu\text{m}$
W_M	Matching section width	$560 \mu\text{m}$
L_M	Matching section length	$250 \mu\text{m}$
W_1	Interdigital capacitor width	$290 \mu\text{m}$
L_1	Interdigital capacitor length	$1040 \mu\text{m}$
W_F	CPW feedline width	$30 \mu\text{m}$
G	CPW feedline gap	$25 \mu\text{m}$
H_{Si}	Si substrate thickness	$380 \mu\text{m}$
H_{SiO_2}	SiO ₂ layer thickness	$1.2 \mu\text{m}$
H_{Al}	Al thickness	$0.2 \mu\text{m}$

diagram of the designed antenna with a microbolometer is presented in Figure 6(c). The optimized dimensions for the microbolometer are the same as the previous design.

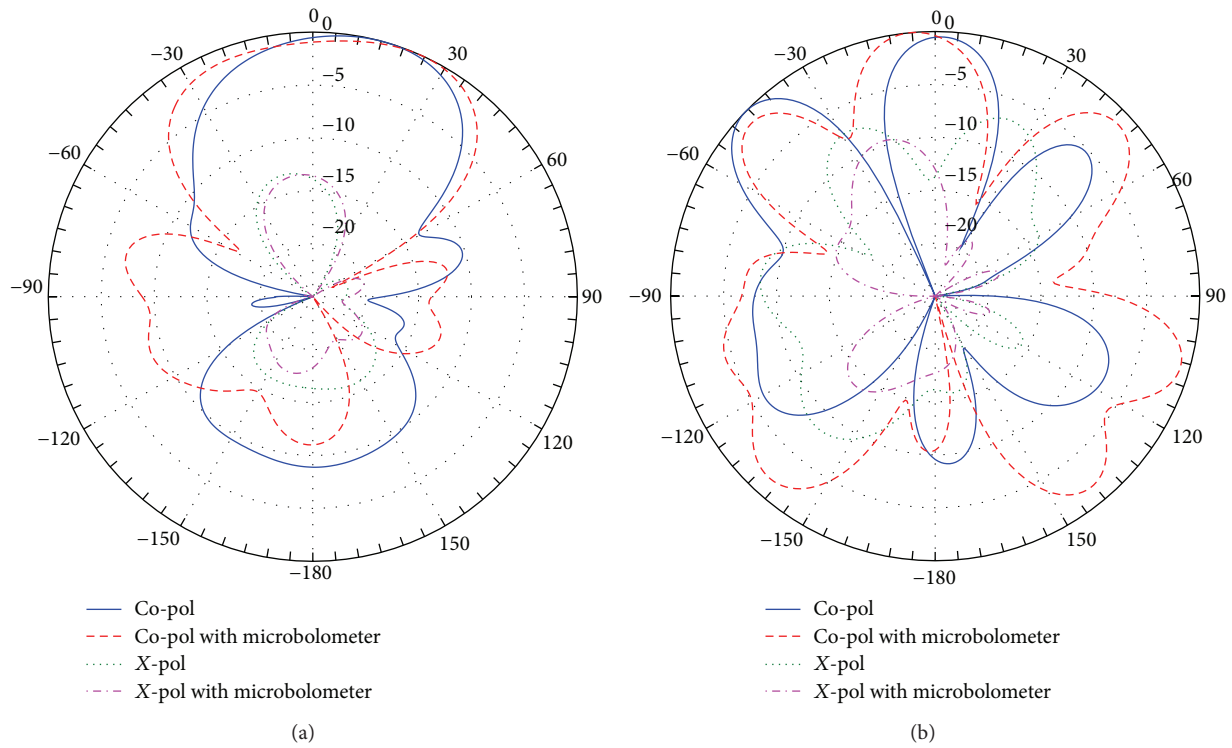


FIGURE 5: Simulated copolarization and cross-polarization radiation patterns in (a) YZ plane and (b) XY plane at $f = 94$ GHz for the Quasi-Yagi loop array antenna prototype I with and without microbolometer.

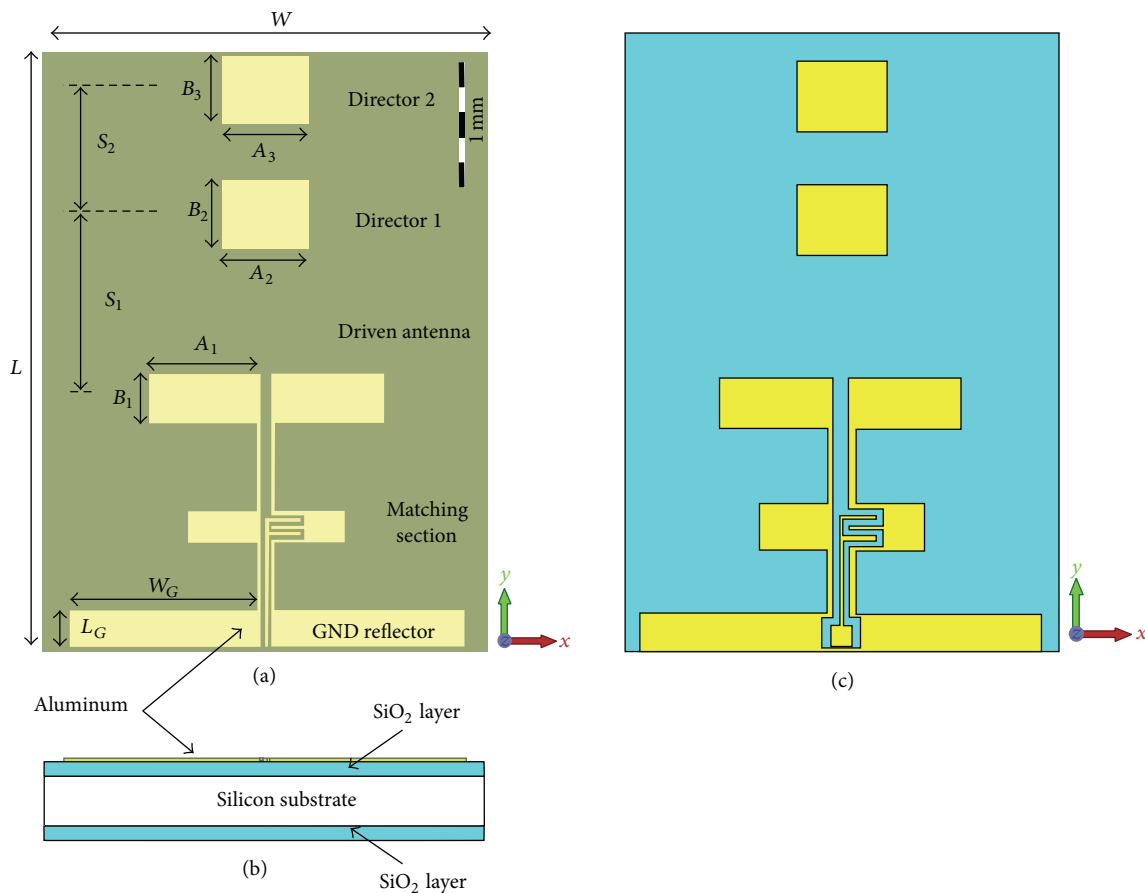


FIGURE 6: Geometrical configuration and photograph of the fabricated Quasi-Yagi dipole antenna prototype II: (a) top view, (b) side view, and (c) schematic diagram of the designed antenna with a microbolometer.

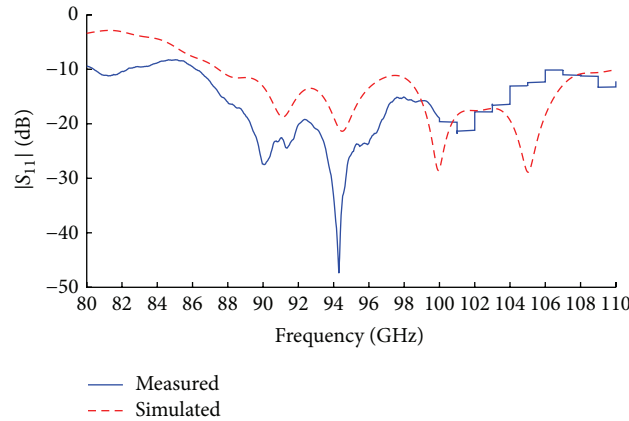


FIGURE 7: Measured and simulated reflection coefficient $|S_{11}|$ versus frequency of proposed Quasi-Yagi dipole antenna prototype II.

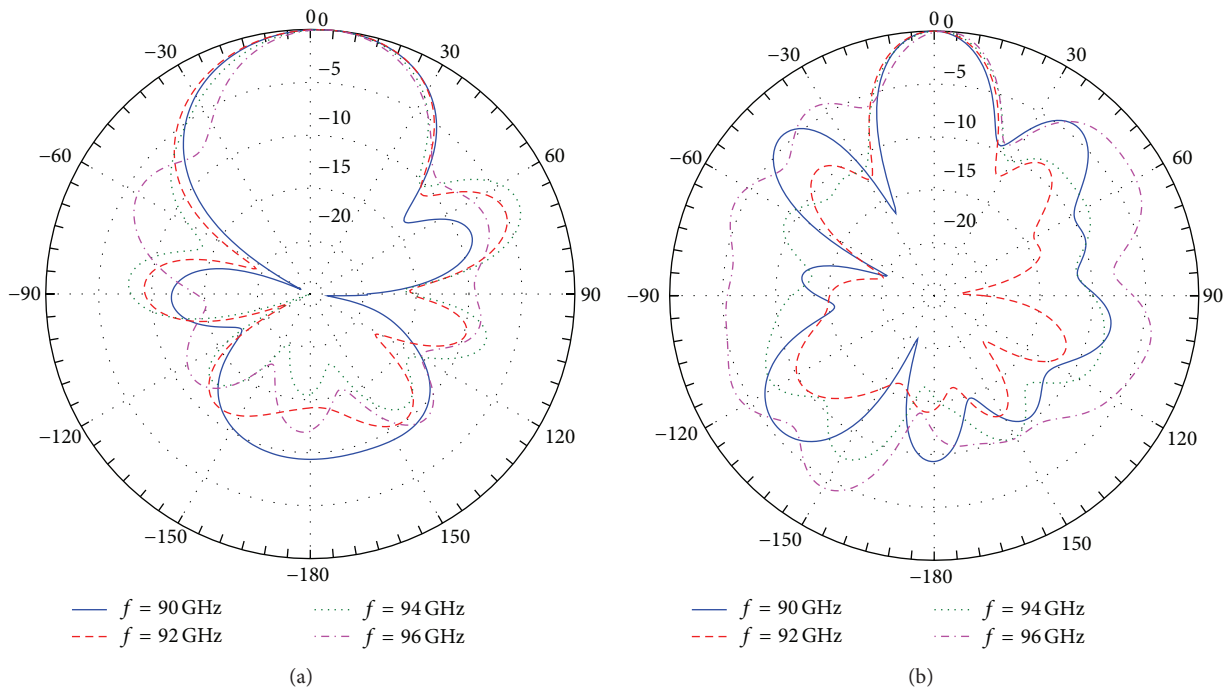


FIGURE 8: Simulated radiation patterns in (a) YZ plane and (b) XY plane at different frequencies $f = 90, 92, 94,$ and 96 GHz for the Quasi-Yagi dipole array antenna prototype II.

3.2. *Measured and Simulated Results.* Figure 7 presents the measured and simulated $|S_{11}|$ results for the antenna prototype II. The results show that there is a good agreement between the measured and simulated one. The antenna exhibits a good -10 dB impedance matching bandwidth starting from 86 GHz to beyond 110 GHz with $|S_{11}|$ value better than -48 dB at 94 GHz.

The simulated antenna radiation patterns are also calculated and presented in Figure 8. The copolarization and cross-polarization components in both XY ($\theta = 90^\circ$) and YZ ($\phi = 90^\circ$) planes at 94 GHz are presented in Figures 8(a) and 8(b), respectively. As shown in the figure, good radiation patterns are achieved with maximum cross-polarization levels of -14.2 dB and -14.8 dB at 94 GHz in both XY and YZ planes,

respectively. The antenna also exhibits a maximum gain of 7.5 dBi and side lobe level of -8.8 dB at frequency of 94 GHz. The 3 dB beam width is found to be approximately 53.8° ; furthermore, the antenna front-to-back ratio of 15.74 dB is achieved.

The simulated copolarization and cross-polarization radiation patterns in both YZ plane and XY plane at $f = 94$ GHz for the Quasi-Yagi dipole array antenna prototype II with and without microbolometer are shown in Figure 9.

Figure 10 presents the peak-realized gain of the two proposed antenna designs. The peak-realized gain of the proposed antenna II is higher than that of the proposed antenna I for the whole frequency band of operation. The calculated antenna radiation efficiencies are found to be

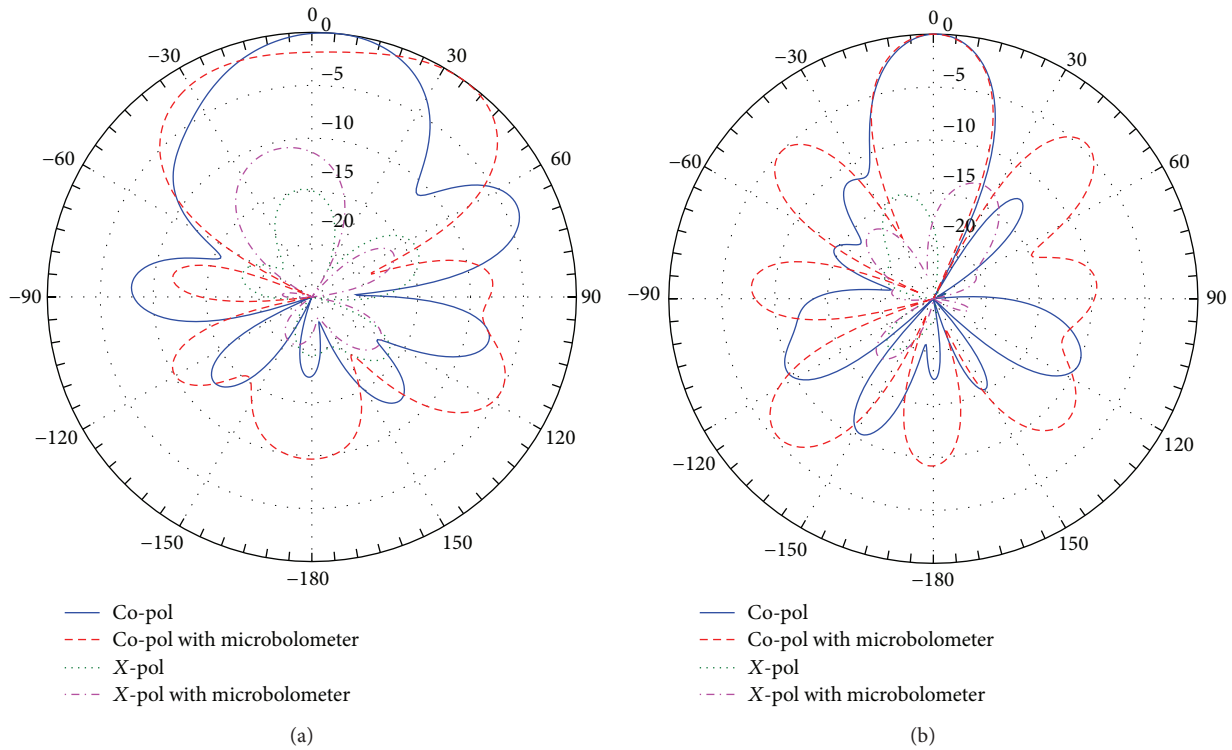


FIGURE 9: Simulated copolarization and cross-polarization radiation patterns in (a) YZ plane and (b) XY plane at $f = 94$ GHz for the Quasi-Yagi dipole array antenna prototype II with and without microbolometer.

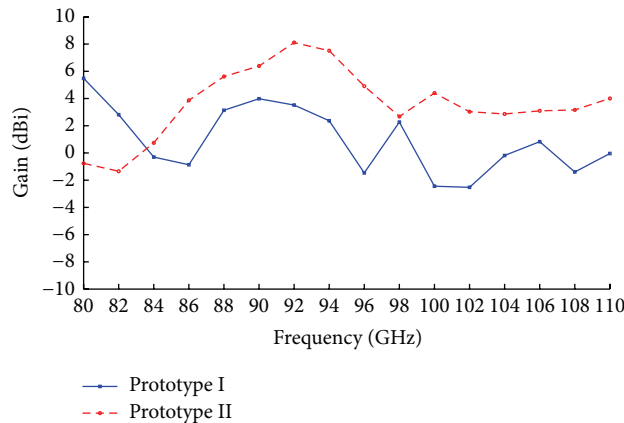


FIGURE 10: Simulated peak-realized gain versus frequency of the proposed Quasi-Yagi antenna prototypes I and II.

approximately ranging from 59% to 88% for the proposed antenna I and from 52% to 77% for the proposed antenna II throughout the band of interest.

3.3. Comparison with Other Related Work. Table 3 presents the performance comparison of other related on-chip Yagi antenna designs reported in the literature. The proposed antenna designs have good performance compared to the other work.

4. Conclusion

Two Quasi-Yagi antenna designs on silicon substrates at 94 GHz for imaging applications have been designed, fabricated, and then tested. The first design uses a driven element of an elliptical shaped loop antenna with elliptical shaped loop directors in front of the driven antenna. The other design utilizes dipole antenna with rectangular shaped patch directors in front of it. The paper also introduces a novel antenna-feed and matching configuration that facilitates

TABLE 3: Performance comparison with other related work in the literature.

Reference	Process technology	Frequency	Gain	Efficiency
[4]	0.18 μm CMOS	60 GHz	-10.6 dBi (measured)	10%
[14]	0.18 μm CMOS	60 GHz	-2.64 dBi (simulated)	16.8%
[16]	Post-back-end-of-line	65 GHz	-12.5 dBi (measured)	5.6%
[17]	Silicon substrate	100 GHz	5.7 dBi (measured)	—
This work	Silicon substrate	94 GHz	7.5 dB (simulated)	59%

coupling a microbolometer element to the developed Quasi-Yagi antenna designs. The proposed antenna-coupled microbolometer design will permit carrying out radiation pattern measurements for the proposed Quasi-Yagi antennas. The impedance bandwidth of more than 24 GHz is achieved at center frequency of 94 GHz with a very reasonable gain of above 4 dBi and 8.1 dBi for prototypes I and II, respectively, throughout the whole band of operation. The antenna radiation efficiencies are found to be between 59% and 88% for the proposed antenna I and 52% and 77% for the proposed antenna II.

Conflict of Interests

The authors declare that there is no conflict of interests regarding the publication of this paper.

Acknowledgment

This research is supported by King Abdul Aziz City for Science and Technology (KACST) Technology Innovation Center in RF and Photonics for the e-Society (RFTONICS) hosted at King Saud University.

References

- [1] H. Yagi, "Beam transmission of the ultra-short waves," *Proceedings of the IRE*, vol. 16, pp. 715–741, 1982.
- [2] R. A. Alhalabi and G. M. Rebeiz, "Differentially-fed millimeter-wave Yagi-Uda antennas with folded dipole feed," *IEEE Transactions on Antennas and Propagation*, vol. 58, no. 3, pp. 966–969, 2010.
- [3] H. Chu, Y.-X. Guo, H. Wong, and X. Shi, "Wideband self-complementary Quasi-Yagi antenna for millimeter-wave systems," *Antennas and Wireless Propagation Letters, IEEE*, vol. 10, pp. 322–325, 2011.
- [4] S.-S. Hsu, K.-C. Wei, C.-Y. Hsu, and H. Ru-Chuang, "A 60-GHz millimeter-wave CPW-fed Yagi antenna fabricated by using 0.18- μm CMOS technology," *IEEE Electron Device Letters*, vol. 29, no. 6, pp. 625–627, 2008.
- [5] J. Yeo and J. I. Lee, "Series-fed two dipole array antenna using bow-tie elements with enhanced gain and front-to-back ratio," *Journal of Electromagnetic Waves and Applications*, vol. 26, no. 11-12, pp. 1641–1649, 2012.
- [6] D. Li and J.-F. Mao, "A Koch-like sided fractal bow-tie dipole antenna," *IEEE Transactions on Antennas and Propagation*, vol. 60, no. 5, pp. 2242–2251, 2012.
- [7] Y. Ding, Y. Jiao, B. Li, and L. Zhang, "Folded triple-frequency quasi-Yagi-type antenna with modified CPW-to-CPS transition," *Progress in Electromagnetics Research Letters*, vol. 37, pp. 143–152, 2013.
- [8] S. X. Ta, B. Kim, H. Choo, and I. Park, "Wideband quasi-Yagi antenna fed by microstrip-to-slotline transition," *Microwave and Optical Technology Letters*, vol. 54, no. 1, pp. 150–153, 2012.
- [9] N. Nikolic and A. R. Weily, "Compact E-band planar quasi-Yagi antenna with folded dipole driver," *IET Microwaves, Antennas and Propagation*, vol. 4, no. 11, pp. 1728–1734, 2010.
- [10] B.-K. Tan, G. Yassin, S. Withington, and D. Goldie, "Broadband planar Yagi antenna for millimetre & sub-millimetre detectors," in *Proceedings of the 6th UK, Europe, China Millimeter Waves and THz Technology Workshop (UCMMT '13)*, pp. 1–2, Rome, Italy, September 2013.
- [11] V. H. Bui and N. C. Dao, "A GA-based optimized broadband millimeter-wave quasi-Yagi antenna," in *Proceedings of the 3rd International Conference on Communications and Electronics (ICCE '10)*, pp. 352–356, NHA Trang, Vietnam, August 2010.
- [12] Y. N. Wijayanto, H. Murata, and Y. Okamura, "Electro-optic wireless millimeter-wave-lightwave signal converters using planar Yagi-Uda array antennas coupled to resonant electrodes," in *Proceedings of the 17th Opto-Electronics and Communications Conference (OECC '12)*, pp. 543–544, Busan, Republic of Korea, July 2012.
- [13] F. Qin, Y. Gao, G. Wei, and J. Xu, "A broadband planar quasi-Yagi antenna with X-shaped driven elements," in *Proceedings of the 8th International Symposium on Communication Systems, Networks & Digital Signal Processing (CSNDSP '12)*, pp. 1–4, Poznan, Poland, July 2012.
- [14] X. Bao, Y. Guo, and S. Hu, "A 60-GHz differential on-chip Yagi antenna using 0.18- μm CMOS technology," in *Proceedings of the IEEE Asia-Pacific Conference on Antennas and Propagation (APCAP '12)*, pp. 277–278, August 2012.
- [15] R. Willmot, D. Kim, and D. Peroulis, "A Yagi-Uda array of high-efficiency wire-bond antennas for on-chip radio applications," *IEEE Transactions on Microwave Theory and Techniques*, vol. 57, no. 12, pp. 3315–3321, 2009.
- [16] Y. P. Zhang, M. Sun, and L. H. Guo, "On-chip antennas for 60-GHz radios in silicon technology," *IEEE Transactions on Electron Devices*, vol. 52, no. 7, pp. 1664–1668, 2005.
- [17] M. Sun and Y. P. Zhang, "100-GHz Quasi-Yagi antenna in silicon technology," *IEEE Electron Device Letters*, vol. 28, no. 5, pp. 455–457, 2007.
- [18] "CST Microwave Studio, Ver. 2012," Framingham, Mass, USA, 2012.

